CANCER

Identification of human CD4$^+$ T cell populations with distinct antitumor activity

Michelle H. Nelson[1,2]*, Hannah M. Knochelmann[1,2]*, Stefanie R. Bailey[1,2], Logan W. Huff[1,2], Jacob S. Bowers[1,2], Kinga Majchrzak-Kuligowska[1,2], Megan M. Wyatt[1,2], Mark P. Rubinstein[1,3], Shikhar Mehrotra[1,3], Michael I. Nishimura[4], Kent E. Armeson[5], Paul G. Giresi[6], Michael J. Zilliox[7], Hal E. Broxmeyer[8], Chrystal M. Paulos[1,2†‡]

How naturally arising human CD4$^+$ T helper subsets affect cancer immunotherapy is unclear. We reported that human CD4$^+$CD26^{high} T cells elicit potent immunity against solid tumors. As CD26^{high} T cells are often categorized as T_H17 cells for their IL-17 production and high CD26 expression, we posited these populations would have similar molecular properties. Here, we reveal that CD26^{high} T cells are epigenetically and transcriptionally distinct from T_H17 cells. Of clinical importance, CD26^{high} and T_H17 cells engineered with a chimeric antigen receptor (CAR) regressed large human tumors to a greater extent than enriched T_H1 or T_H2 cells. Only human CD26^{high} T cells mediated curative responses, even when redirected with a suboptimal CAR and without aid by CD8$^+$ CAR T cells. CD26^{high} T cells cosecreted effector cytokines, produced cytotoxic molecules, and persisted long term. Collectively, our work underscores the promise of CD4$^+$ T cell populations to improve durability of solid tumor therapies.

INTRODUCTION

CD26 is a surface glycoprotein expressed on various cell types, including fibroblasts, epithelial, and immune cells (*1*). CD26 has many properties that could influence T cell function, including enzymatic cleavage of chemokines that regulate migration (*2*) to costimulation via caveolin-1 (*3*, *4*). CD26$^+$ T cells have been associated with exacerbating various autoimmune manifestations and augmenting antitumor immunity (*5*–*9*). We reported that CD26 distinguishes three human CD4$^+$ T cell subsets with varying degrees of responsiveness to tumors: one with regulatory properties (CD26^{neg}), one with a naïve/central memory phenotype (CD26^{int}), and one with a durable stem memory profile (CD26^{high}) (*9*). Adoptively transferred CD26^{high} T cells engineered with chimeric antigen receptors (CARs) persisted and regressed difficult-to-treat malignancies superior to CD26^{neg} T cells and, unexpectedly, slightly better than naïve CD26^{int} T cells. CD26^{high} T cells secreted T helper cell 17 (T_H17) cytokines, including interleukin-17A (IL-17A). These findings suggest CD4$^+$CD26^{high} T cells are promising for immunotherapies.

Yet, the clinical potential of naturally arising human CD4$^+$ T helper subsets sorted from the peripheral blood via classic surface markers and engineered with a CAR has yet to be elucidated. The potency of murine T_H17 cells over T_H1 or T_H2 cells in tumor immunity has been reported by many groups (*10*–*13*). However, the impact of human T_H17 cells in the context of adoptive T cell transfer (ACT) therapy has not been fully explored. Given that CD26^{high} cells express master transcription factor (TF) RORγt and produce IL-17 (*14*), we postulated that human CD26^{high} T cells would regress tumors to the same extent as classic T_H17 cells (i.e., CCR4$^+$CCR6$^+$CD4$^+$) relative to other CD4$^+$ subsets when redirected with a CAR and infused into hosts bearing human tumors (*15*).

After deep sequencing and direct functional analysis of these subsets, we report that CD26^{high} T cells are molecularly and functionally distinct from T_H17 cells. While both CD26^{high} and T_H17 cells were therapeutic in murine models, human CD26^{high} T cells mediated durable, relapse-free immunity, while bulk CD4, T_H1, T_H2, or T_H17 cell therapies elicited only transient delays in human tumor growth. Human CD26^{high} T cells demonstrated the highest engraftment and persistence in the peripheral blood and in tumors. Additional investigation revealed that IL-17 and high surface CD26 were not required for tumor regression nor were cotransferred CD8$^+$ T cells, suggesting that unique molecular and epigenetic properties may play a role in the potency of human CD26^{high} T cells. This paper represents an important advancement in our understanding of targeting human CD4$^+$ T cell subsets to tumors and has profound implications for future cancer immunotherapies.

RESULTS

CD26^{high} T cells have a dynamic cytokine profile

We reported that CD4$^+$ T cells expressing high CD26 levels (termed CD26^{high} T cells) secrete IL-17A and elicit potent tumor immunity when redirected with a CAR compared with sorted CD26^{int} or CD26^{low} T cells (*9*). While CD26^{high} T cells are categorized as T_H17 cells, the functional profile of sorted human CD26^{high} T cells compared with classic T_H17 cells and other known helper subsets has not been formally tested. Given the abundance of IL-17 produced by CD26^{high} T cells and the reported high CD26 expression on T_H17 cells (*14*), we suspected that CD26^{high} T cells would have a similar cytokine profile as classic T_H17 cells. To first address this question, we measured the level and type of cytokines produced by various CD4$^+$ subsets. These subsets were sorted from the peripheral blood of healthy

[1]Department of Microbiology and Immunology, Medical University of South Carolina, Charleston, SC, USA. [2]Department of Dermatology and Dermatologic Surgery, Medical University of South Carolina, SC, USA. [3]Department of Surgery, Medical University of South Carolina, Charleston, SC, USA. [4]Department of Surgery, Stritch School of Medicine, Loyola University Chicago, Maywood, IL, USA. [5]Department of Public Health Sciences, Medical University of South Carolina, Charleston, SC, USA. [6]Epinomics, Menlo Park, CA, USA. [7]Department of Public Health Sciences, Stritch School of Medicine, Loyola University Chicago, Maywood, IL, USA. [8]Department of Microbiology and Immunology, Indiana University School of Medicine, Indianapolis, IN, USA.
*These authors contributed equally to this work.
†Present address: Department of Surgery and Department of Microbiology and Immunology, Winship Cancer Institute, Emory University School of Medicine, Atlanta, GA 30322, USA.
‡Corresponding author. Email: paulos@musc.edu, paulos@emory.edu

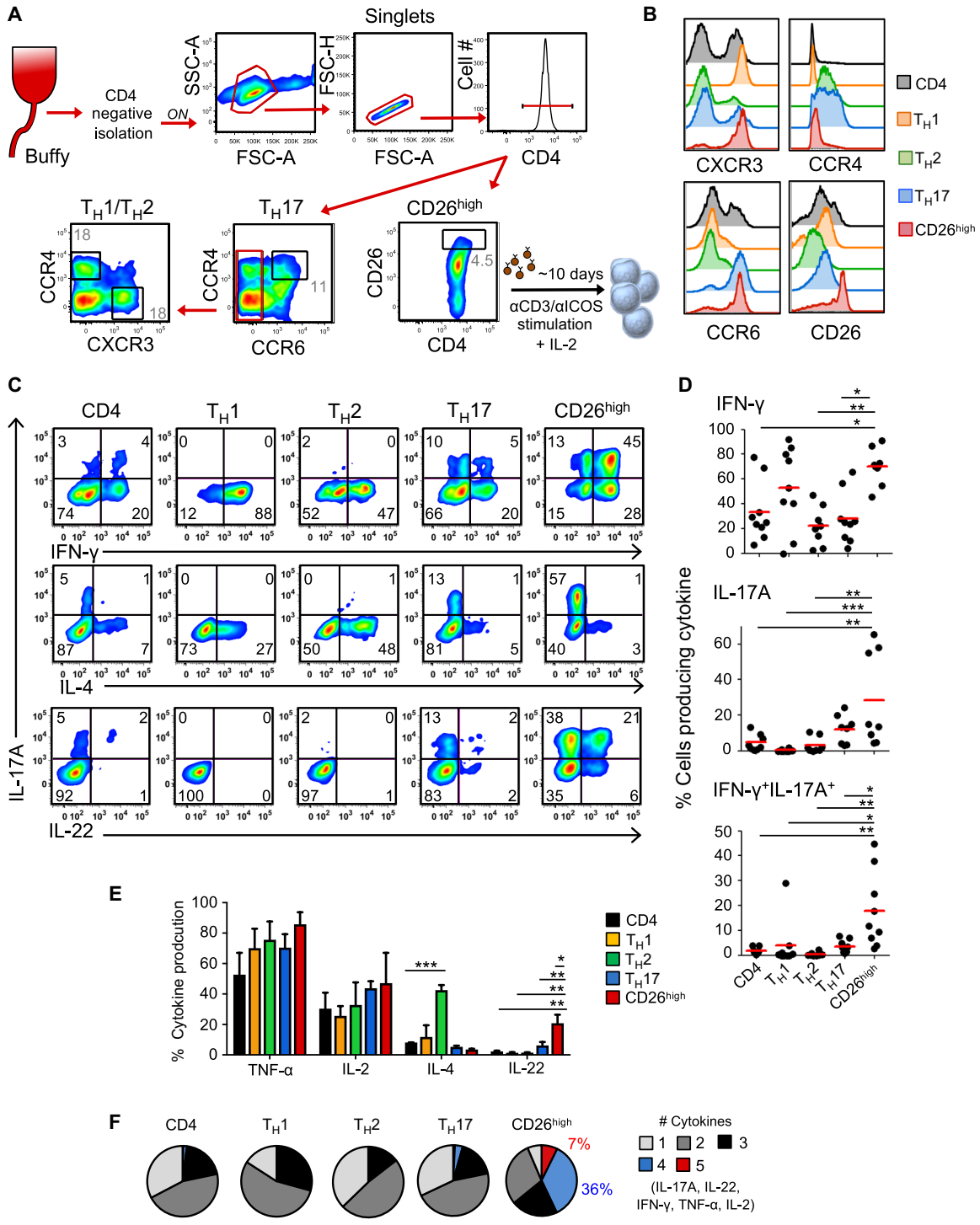

Fig. 1. CD4$^+$CD26^{high} T cells have a dynamic cytokine profile. (**A**) CD4$^+$ subset sorting scheme. CD4$^+$ lymphocytes were negatively isolated using magnetic beads from normal donor peripheral blood lymphocytes (PBLs). T_H17 cells were sorted from the CCR6$^+$CCR4$^+$ gate. T_H1 and T_H2 cells are both CCR6$^-$ and subsequently sorted via CXCR3 or CCR4, respectively. CD26^{high} cells were sorted independently on the basis of CD26 expression. (**B**) Chemokine receptor profile after sort. (**C**) CD4$^+$ T cell subsets were stimulated with αCD3/inducible costimulator (ICOS) beads at a ratio of 1 bead:10 T cells and expanded in IL-2 (100 IU/ml). Ten days following activation, the five different cell subsets were examined for their intracellular cytokine production. Dot plot representation of IL-17, interferon-γ (IFN-γ), IL-4, and IL-22 expression by flow cytometry. (**D**) Graphical representation of at least eight normal donors from independent experiments demonstrating IFN-γ and IL-17 single and double producing cells by flow cytometry. (**E**) Graphical representation of 10 normal donors demonstrating cytokine-producing cells by flow cytometry. Two to three replicates each. Analysis of variance (ANOVA), Tukey's post hoc comparisons; *$P < 0.05$, **$P < 0.01$, and ***$P < 0.001$. (**F**) Cells were gated on cytokine-producing cells to quantify cells that produced between one and five cytokines simultaneously. Cytokines of interest were IL-17, IFN-γ, IL-2, IL-22, and tumor necrosis factor–α (TNF-α). Representative of five experiments.

individuals via extracellular markers (Fig. 1A) (*15*). This sort yielded T_H1 ($CXCR3^+CCR4^-CCR6^-$), T_H2 ($CXCR3^-CCR4^+CCR6^-$), T_H17 ($CCR4^+CCR6^+CXCR3^{+/-}$), and $CD26^{high}$ T cells with high purity (>90%). Flow cytometry validated that enriched T_H1 cells expressed CXCR3, while T_H2 cells expressed CCR4, and T_H17 cells coexpressed CCR4 and CCR6. $CD26^{high}$ T cells also expressed high CXCR3 and CCR6 but nominal CCR4 on their surface (Fig. 1B). As previously reported, T_H17 cells expressed more CD26 than other subsets (Fig. 1B) (*14*).

After assessing cytokine production, we found that $CD26^{high}$ T cells were not restricted to a T_H17-like functional profile (Fig. 1C). Instead, $CD26^{high}$ T cells secreted comparable amounts of IL-17A and greater levels of interferon-γ (IFN-γ) and IL-22 than T_H17 cells (Fig. 1, C to E). $CD26^{high}$ T cells produced nearly as much IFN-γ as T_H1 cells but less IL-4 than T_H2 cells. We consistently observed this functional pattern in $CD26^{high}$ T cells from several healthy individuals (Fig. 1C to E). On a per-cell basis, these various $CD4^+$ T cell populations were assayed for their capacity to secrete up to five cytokines at once, including IL-17A, IL-22, IFN-γ, tumor necrosis factor–α (TNF-α), and IL-2 (Fig. 1F). Only $CD26^{high}$ T cells secreted four (36%) to five (7%) cytokines simultaneously, while bulk $CD4^+$, T_H1, T_H2, and T_H17 cells, at most, cosecreted three cytokines (Fig. 1F).

As $CD26^{high}$ T cells express more IL-23R mRNA than $CD26^{low}$ or $CD26^{int}$ T cells (*9*, *14*), we tested whether this cytokine would induce T_H1 or T_H17 cells to cosecrete elevated IL-17A and IFN-γ to the levels mediated by $CD26^{high}$ T cells. While IL-23 did not provoke T_H1 cells to cosecrete IL-17A and IFN-γ, it did increase the coproduction of these two cytokines by T_H17 cells (fig. S1, A and B), albeit not to the extent of $CD26^{high}$ T cells. Overall, $CD26^{high}$ T cells have a functional profile distinct from other $CD4^+$ T subsets and are more dynamic than classic T_H17 cells.

$CD26^{high}$ T cells display a unique chromatin landscape

Given the functional profile of $CD26^{high}$ T cells, we hypothesized that the epigenetic landscape of these cells at resting state would be different from that of T_H17 cells. To test this idea, we sorted naïve, T_H1, T_H2, T_H17, and $CD26^{high}$ T cells from the blood of five different healthy donors and profiled their chromatin accessibility with assay for transposase-accessible chromatin with high-throughput sequencing (ATAC-seq). $CD26^{high}$ T cells contained peaks displaying enhancer-accessible regions near various TFs known to direct T_H1 (such as *Tbx21* and *EOMES*) and T_H17 (*RORC*) cell lineage development while displaying suppressor regions near TF genes known to regulate T_H2 development, such as *GATA3* (Fig. 2, A and B). While *Tbx21* and *EOMES* were more accessible in both T_H1 and $CD26^{high}$ T cells, they were repressed in naïve, T_H2, and T_H17 cells (Fig. 2B). Moreover, a core of other accessible regions in T_H1-related TFs, such as *MGA*, *STAT2*, *STAT1*, and *STAT5A*, were pronounced in T_H1 and $CD26^{high}$ T cells (Fig. 2A). As expected, accessible regions surrounding *GATA3* were enhanced in T_H2 cells and T_H17 cells. Other enhancer accessible regions surrounding T_H2-like TFs, such as *GATA1*, *GATA2*, *GATA4*, *GATA5*, *GATA6*, *PAX4*, *YY1*, *PITX2*, and *GFI1*, were distinguished in T_H2 and T_H17 cells (Fig. 2A). Similar to T_H17 cells, chromatin-accessible regions near the *RORA*, *RORC*, and *STAT3* loci were enhanced in $CD26^{high}$ T cells but suppressed in naïve, T_H1, and T_H2 cells (Fig. 2, A and B). T_H1 cells more closely aligned with the epigenetic landscape of naïve cells, as they both expressed accessible chromatin regions neighboring TFs in the stem and development pathways, including *TCF7*, *LEF1*, *CTCF*, *DNMT1*, and *ZFP161* (Fig. 2A). Yet, certain accessible regions in naïve cells were also heightened in both $CD26^{high}$ and T_H1 subsets, including *STAT1*, *STAT2*, *IRF1*, *IRF2*, *IRF3*, *IRF5*, *IRF7*, *IRF8*, and *ZNF683* (Fig. 2A).

Despite overlap with T_H1 and T_H17 cells, $CD26^{high}$ T cells had a unique set of differentially accessible elements relative to other subsets. Open accessible regions in the CCAAT/enhancer-binding protein family (C/EBP), which function as TFs in processes including cell differentiation, motility, and metabolism were among the most unique and differentially expressed in $CD26^{high}$ T cells (Fig. 2, A and B). Along with *CEBPs*, *ELK3*, important for cell migration and invasion, and *RUNX*, which promotes memory cell formation, were enhanced in $CD26^{high}$ T cells. Principal components analysis of the genome-wide open chromatin landscape of these 25 samples showed that $CD26^{high}$ T cells cluster separately from naïve, T_H1, T_H2, and T_H17 cells (Fig. 2C). We verified the distinct characteristics of $CD26^{high}$ versus T_H17 cells using gene array (fig. S2, A and B). Further, as helper subsets have been reported to express a particular β T cell receptor (TCRβ) repertoire (*16*), we defined the frequency and likelihood of TCRβ-clonotype overlap between various sorted subsets and found nominal overlap between $CD26^{high}$ cells and other helper subsets (Fig. 2D and fig. S2C). Collectively, we conclude that the epigenetic landscape and TCR repertoire of $CD26^{high}$ cells differ substantially from that of classic $CD4^+$ subsets.

Single-cell sequencing reveals that $CD26^{high}$ T cells are molecularly unique from T_H17 cells

Single-cell transcriptome analysis also supported that $CD26^{high}$ T cells are distinguished from T_H17 cells on the basis of differential clustering from that of bulk $CD4^+$ and T_H17 cells (Fig. 3A). A cluster of regulatory T cell (T_{reg})–like cells was present within the sorted T_H17 population (Fig. 3B), as demonstrated by heightened *FOXP3*, *IL2RA*, and *TIGIT* and reduced *IL7R* transcript, but was not found within $CD26^{high}$ T cells. A small cluster of T_H1-like cells was identified within the sorted bulk $CD4^+$ population, as indicated by elevated *TBX21* and *CXCR3* but nominal transcripts associated with T_H17 or T_{reg} cells, such as *CXCR6*, *CCR6*, *CCR4*, *RORC*, and *FOXP3*. Transcripts associated with less differentiated populations, composed of naïve or central memory cells, including *SELL*, *CCR7*, and *CD27*, were expressed at slightly higher levels in bulk $CD4^+$ cells than other populations. Conversely, *IL2RB* and *IL15RA* were lower on bulk $CD4^+$ T cells compared with other populations. In concurrence with their chromatin accessibility, *CEBPD* transcripts were elevated in $CD26^{high}$ T cells compared with bulk $CD4^+$ or T_H17 cells. Together, these data suggest that $CD26^{high}$ T cells are unique from T_H17 cells, yet their relative clinical potential in cancer immunotherapy remained unknown.

$CD26^{high}$ T cells demonstrate enhanced tumor immunity compared with other helper subsets

We reported that T_H17 cells cosecrete more IL-17A and IFN-γ after expansion with CD3/inducible costimulator (ICOS) versus CD3/CD28 activator beads (*17*). While CD3/CD28 beads are mainly used to manufacture CAR T cell products, we and others (*18*) have found that the frequency of T_{regs} is augmented in $CD4^+$ cultures expanded with CD3/CD28 beads relative to CD3/ICOS beads (fig. S3A). Moreover, T_H1, T_H17, and $CD26^{high}$ cells secreted elevated IFN-γ and/or IL-17A when expanded with CD3/ICOS beads compared with CD3/CD28 beads (fig. S3B). Therefore, we elected to use the CD3/ICOS bead expansion platform to investigate the relative antitumor potential of various sorted $CD4^+$ T helper populations in vivo. Specifically, as in fig. S4A, we engineered sorted T_H1, T_H2, T_H17, $CD26^{high}$,

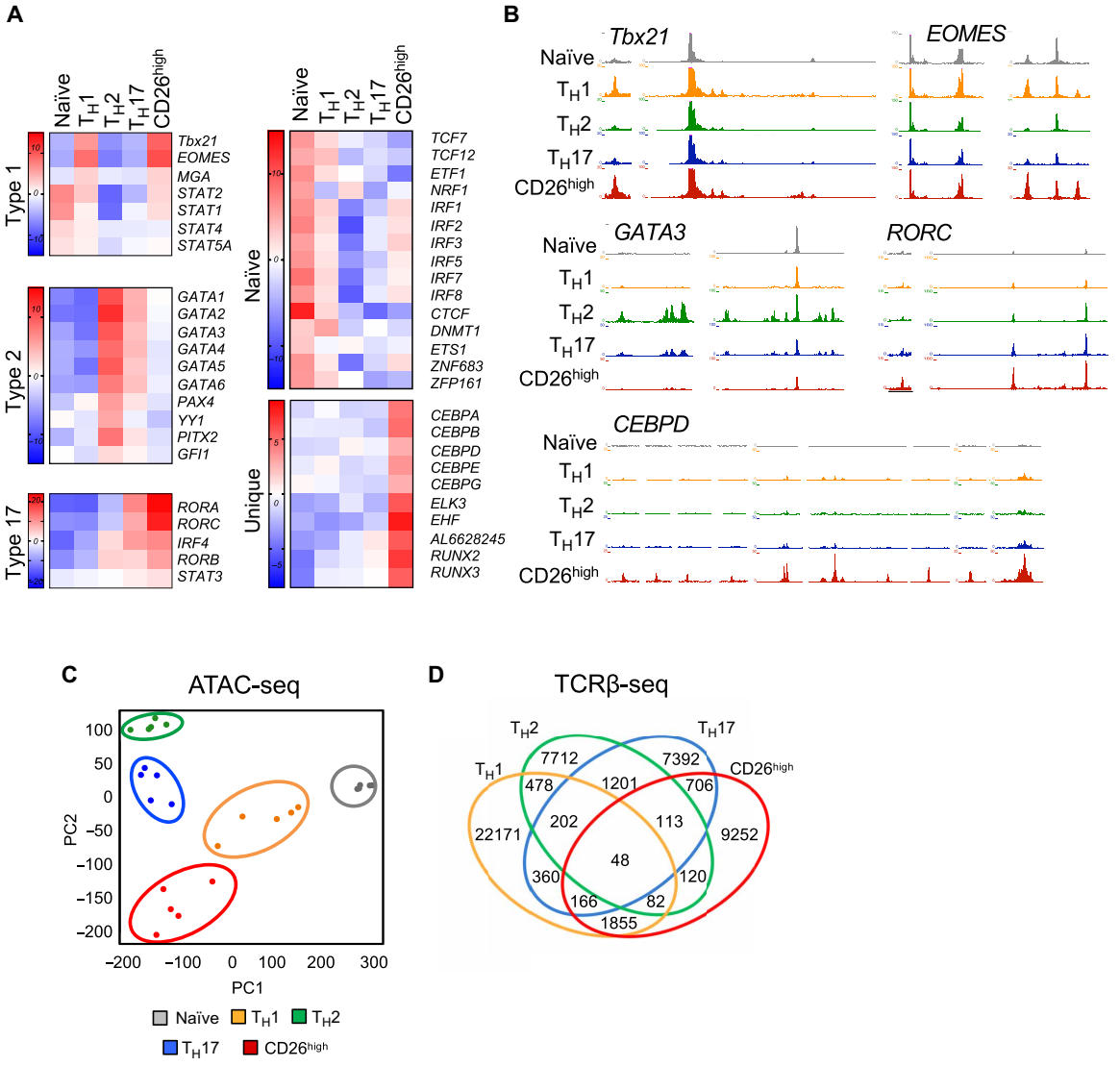

Fig. 2. The epigenetic and molecular signature of CD26^{high} T cells are unique. (**A**) ATAC-seq analysis describing chromatin accessibility in FACS (fluorescence-activated cell sorting)–sorted CD4$^+$ subsets (naïve, T_H1, T_H2, T_H17, and CD26^{high}) organized by TF networks known to describe T_H1, T_H2, T_H17, and naïve subsets. Accessible transcription regions unique to CD26^{high} T cells are also shown. Compiled from five healthy donors. (**B**) UCSC genome browser tracks for sorted CD4$^+$ subsets around classical T helper TFs from ATAC-seq analysis. (**C**) ATAC-seq principal components analysis of sorted T cell subsets analyzed at resting state. $n = 5$ donors. (**D**) β T cell receptor (TCRβ) sequencing of CD26^{high}, T_H17, and T_H1 cells sorted from peripheral blood of healthy donors demonstrates unique or shared clonotypes. Venn diagram illustrates percentage of unique or shared TCRβ sequences. The relative frequencies (standardized to sum to 1.0): CD26^{high} only = 0.237, T_H1 only = 0.487, T_H17 only = 0.196, CD26^{high} and T_H1 = 0.041, CD26^{high} and T_H17 = 0.020, T_H1 and T_H17 = 0.015, and all three = 0.004, log-linear model.

and bulk CD4$^+$ T cells to express mesothelin-specific CAR (meso-CAR) and infused them into NSG (nonobese diabetic, severe combined immunodeficient gamma chain knockout) mice bearing large established mesothelioma tumors. Note that we used a first-generation meso-CAR, reported by our colleagues to be less therapeutic than second-generation meso-CARs (*19*), as we surmised this approach would generate a treatment window to address whether CD26^{high} T cells lyse tumor to a greater extent than other subsets. CD8$^+$ T cells (10-day expanded) were also redirected with this first-generation CAR and coinfused at equal numbers with these various CAR-CD4$^+$ subsets (Fig. 4A). CD26^{high} T cells eradicated tumors, while T_H17 cells only regressed tumors short term (Fig. 4, B and C). Yet, both CD26^{high} and T_H17 cells were more effective than T_H1, T_H2, or bulk CD4$^+$ T cells (Fig. 4, B and C). Ultimately, mice treated with CD26^{high} T cells survived significantly longer (Fig. 4D), which was associated with higher CD4$^+$ and CD8$^+$ CAR T cell engraftment and persistence compared with other subsets (Fig. 4, E and F). Moreover, cotransferred CD4$^+$CD26^{high} cells, and T_H17 cells to a lesser extent, improved the function of CD8$^+$ CAR T cells, as persistence of CD8$^+$IFN-γ$^+$ and CD8$^+$IFN-γ$^+$/IL-2$^+$/TNF-α$^+$ CAR T was elevated in the spleen (fig. S4, B to D).

As immunity via CAR therapy was enhanced using T_H17 or CD26^{high} populations over other subsets, we anticipated that IL-17A or CD26 itself regulated their efficacy. However, persisting T_H17 and CD26^{high} CAR T cells did not produce IL-17A but rather secreted more IFN-γ long term after ACT, suggesting IL-17A may not be

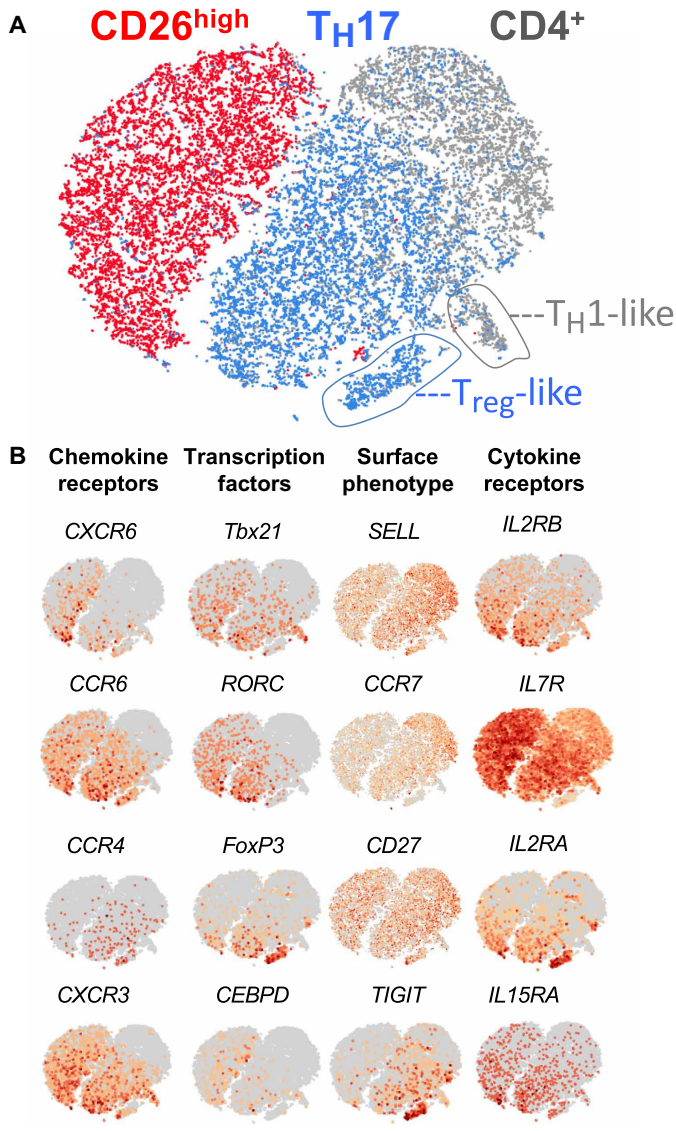

Fig. 3. CD4$^+$CD26^{high} T cells are distinguished from T$_H$17 cells via single-cell sequencing. Total CD4$^+$, CD26^{high}, and T$_H$17 cell subsets were sorted from the peripheral blood of healthy donors, and ~3000 cells were assayed by single-cell RNA sequencing. (**A**) Data were analyzed by t-distributed stochastic neighbor embedding (t-SNE). (**B**) t-SNE plot overlaid with mRNA expression of chemokine receptors, TFs, memory markers, and cytokine receptors. Representative of three healthy donors.

responsible for their maintenance (fig. S4E). Thus, we next tested whether CD26 was critical by knocking it out in CAR T cells via CRISPR-Cas9–mediated genome engineering. To capitalize on cell yield needed for these multiple genetic manipulations, we polarized bulk CD4$^+$ T cells to the T$_H$17 phenotype. These cells were activated, engineered with meso-CAR, knocked out of CD26, and sorted to obtain a pure CD26$^-$ population (fig. S5, A to C). Neither cytokine production nor tumor immunity was affected by loss of CD26 (fig. S5, D to F). Overall, these data imply that IL-17 and CD26 may not be critical to effective antitumor responses mediated by transferred T$_H$17 or CD26^{high} T cells.

We also found that murine tyrosinase-related protein 1 (TRP-1) CD26^{high} and T$_H$17 cells stalled the growth of poorly immunogenic B16F10 melanoma to a greater extent than TRP-1 T$_H$1 cells in mice (fig. S6A). Moreover, murine CD26^{high} T cell therapy enhanced the survival of mice compared with T$_H$1 cells but was not markedly different from T$_H$17 cells (fig. S6B). Our data underscore in two distinct solid tumor models the promise of T$_H$17 and particularly human CD26^{high} T cells in immunotherapy.

CD4$^+$CD26^{high} T cells do not require CD8$^+$ CAR T cells for persistence in the tumor

Given the potency of human meso-CAR CD26^{high} T cell therapy against mesothelioma, we next sought to uncover whether cotransferred CD8$^+$ T cells were important for long-term survival in mice. Because of the polyfunctionality of CD26^{high} cells (Fig. 1), along with their heightened cytotoxic capacity (fig. S7), we posited that they may not require CD8$^+$ CAR T cells. To address this question, CD4$^+$CD26^{high} CAR T cells were transferred with or without CD8$^+$ CAR T cells into mice bearing M108 tumors (fig. S8, A and B). Indeed, CD4$^+$CD26^{high} CAR T cells did not require the presence of CD8$^+$ CAR T cells to regress tumors, and CD8$^+$ CAR T cells alone were not therapeutic long term (fig. S8B).

Last, we questioned whether the CAR signaling in CD4$^+$CD26^{high} cells was critical to improve CD8$^+$ CAR T cell persistence in the tumor or whether their presence alone (i.e., redirected with a nonsignaling CAR) could support CD8$^+$ CAR T cells. To address this question, CD8$^+$ and CD26^{high} T cells were redirected with either a full-length signaling meso-CAR-ζ or a truncated TCRζ domain without signaling capability (Δζ) but could still recognize mesothelin and analyzed their presence in tumors. We found that meso-ζ-CD26^{high} cells, either coinfused with meso-Δζ-CD8$^+$ or with meso-ζ-CD8$^+$ T cells, promoted CD45$^+$ immune persistence in M108 tumors 84 days after transfer (fig. S8C). Conversely, CAR T cells did not persist whether transferred with meso-Δζ-CD26^{high} cells. Collectively, our work reveals that meso-CAR CD4$^+$CD26^{high} cells are cytotoxic, require CD3ζ signaling to survive long term, and regress tumors in the absence of conventional meso-CAR CD8$^+$ T cells.

DISCUSSION

CAR T cells are therapeutic in patients with hematological malignancies but have been largely ineffective in individuals with solid tumors, owing in part to the oppressive tumor microenvironment and poor persistence. Many efforts for overcoming these obstacles include modulating T cell trafficking, cytokine delivery, costimulation, and improving cell persistence among other strategies reviewed previously (*20*). CD4$^+$ T cells help cytotoxic CD8$^+$ T cells and, when CAR engineered, improve longevity of responses against hematological malignancies (*21*, *22*). Here, we reveal that naturally arising CD4$^+$ T cell subsets in the peripheral blood differentially affect efficacy of CAR therapy for solid tumors. For the first time, we demonstrate that CD4$^+$CD26^{high} T cells redirected with CAR have enhanced functional and antitumor activity versus classic human subsets (T$_H$1, T$_H$2, and T$_H$17) or unselected CD4$^+$ T cells, as summarized visually in Fig. 5.

CD26^{high} T cells derived from the peripheral blood of healthy individuals were polyfunctional, cosecreting elevated IL-17A and IFN-γ, while classic T$_H$1, T$_H$2, or T$_H$17 cells lacked this dynamic profile. Moreover, CD26^{high} T cells had epigenetic and molecular properties distinguishing them from T$_H$17 or T$_H$1 cells. Of clinical importance, CD26^{high} T cells persisted and ablated mesothelioma in

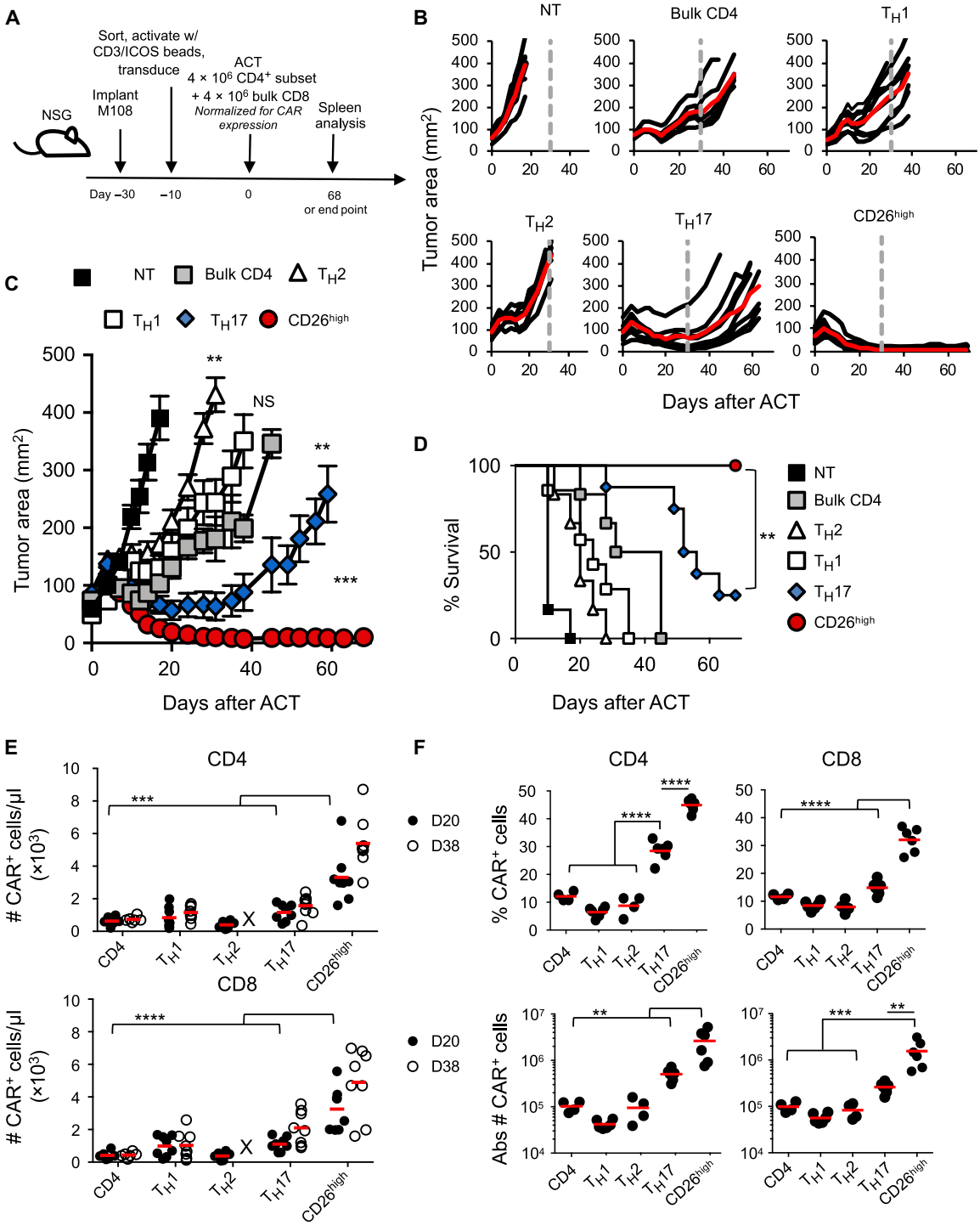

Fig. 4. Human CD26^{high} T cells ablate large human tumors and persist relative to other CD4$^+$ T cell subsets. (**A**) ACT schematic. T_H1 (CXCR3$^+$), T_H2 (CCR4$^+$), T_H17 (CCR4$^+$/CCR6$^+$), CD26^{high}, or bulk CD4$^+$ cells were sorted from normal donor PBL and expanded with αCD3/ICOS beads at a 1 bead:10 T cell ratio. Cells were transduced with a first-generation mesothelin-specific CD3ζ CAR and expanded with IL-2. NSG mice bearing mesothelioma were treated with 4×10^6 transduced, sorted CD4$^+$ cells + 4×10^6 transduced CD8$^+$ cells, and 50,000 IU of IL-2 was given to each mouse daily for 3 days. (**B**) Single-tumor curves overlaid with average curve (red) and (**C**) average tumor curves of six to nine mice per group. All groups were significantly different from non-treated mice (NT), $P < 0.005$. CD4 versus T_H1, NS; CD4 versus T_H2, $^{**}P = 0.0015$; CD4 versus T_H17, $^{**}P = 0.0035$; CD4 versus CD26^{high}, $^{***}P = 0.0003$; T_H17 versus CD26^{high}, $^{**}P = 0.008$; polynomial regression. (**D**) The percentage of mice surviving with tumor size below the 200-mm^2 threshold. Log-rank test. (**E**) Engraftment and persistence of CAR$^+$ T cells in the peripheral blood at days 20 (D20) and 38 (D38) after ACT. $n = 6$ to 8 mice per group. X denotes group was at end point before bleed. (**F**) Spleens were analyzed by flow cytometry for the percentage and total number of CD3$^+$CAR$^+$CD4$^+$ or CD8$^+$ cells at day 68 (T_H17 and CD26^{high}) or group end point (CD4, T_H1, and T_H2). $n = 4$ to 6 mice per group. (E and F) ANOVA, Tukey's post hoc comparisons; $^{**}P < 0.01$, $^{***}P < 0.001$, and $^{****}P < 0.0001$.

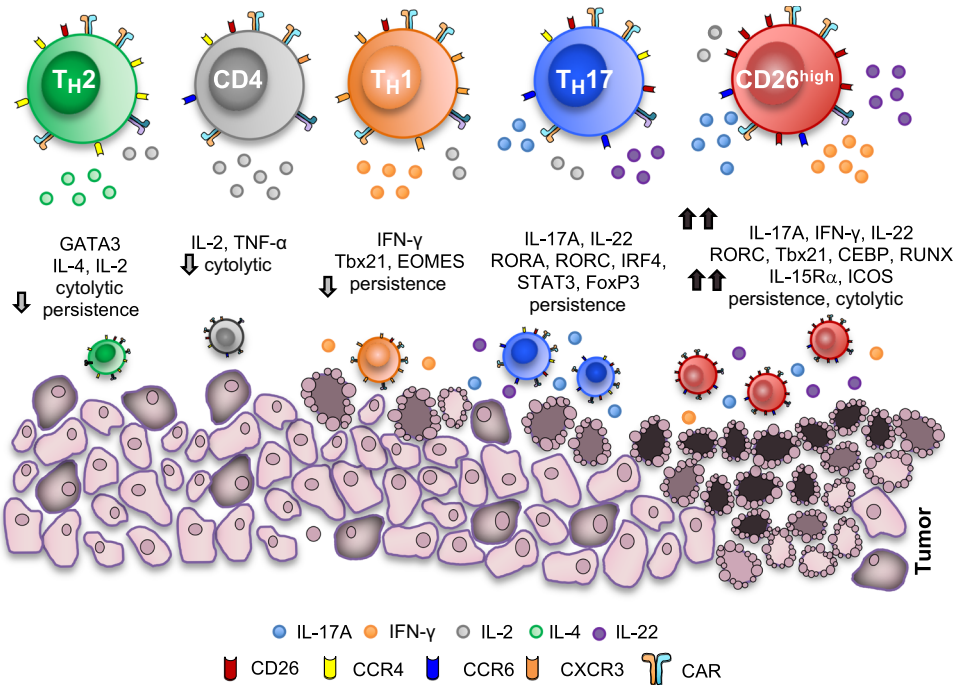

Fig. 5. CD4$^+$CD26^{high} T cells have distinct antitumor and molecular properties relative to other helper subsets. CD26^{high} T cells have been described herein for use in ACT therapy. These cells produce heightened levels of cytokines including IL-17, IFN-γ, IL-22, and IL-2 and can cosecrete these cytokines. CD26^{high} T cells have a distinct chromatin landscape with accessible regions near *RORC*, *Tbx21*, *CEBP*, and *RUNX* TFs and have a unique transcriptional signature. These cells are cytotoxic, multifunctional, and inflammatory. Overall, CD26^{high} T cells persist and regress tumors to a remarkably greater extent than other CD4$^+$ T cells in vivo and represent a distinct CD4$^+$ helper population with potent antitumor properties.

mice when ex vivo engineered with CAR, while T_H17 cell therapies transiently regressed tumors, and bulk CD4$^+$, T_H1, or T_H2 subsets were largely ineffective.

As T_H17 cells express the highest CD26 relative to other subsets, we anticipated that CD26 or IL-17 may be driving antitumor properties in T_H17/CD26^{high} T cell therapies. Unexpectedly, neither of these factors appeared critical to delay tumor growth. CRISPR-Cas9–mediated knockout of CD26 in T_H17 cells delayed the onset of tumor regression but ultimately did not affect the overall antitumor response in mice. In addition, CAR T_H17 or CD26^{high} T cells persisting for several months after ACT did not maintain IL-17 expression but continued to produce IFN-γ. These data suggest that IFN-γ, rather than IL-17, is more important to immunity elicited by T_H17 or CD26^{high} T cells, a concept supported by other models transferring murine IL-17–producing tumor-specific T cells (*10*, *23*).

While CD26 may not directly affect tumor immunity from CD4$^+$ CAR T cells in our NSG human xenograft model, it remains possible that CD26 marks lymphocytes with the ability to persist. CD26^{high} T cells engrafted in the peripheral blood and tissues at early time points after adoptive transfer and remained detectable at the tumor bed for several months. Properties such as their stemness profile, polyfunctionality, or, perhaps, resistance to the oppressive microenvironment may permit their survival within the tumor. Alternately, trafficking of CD26^{high} T cells may support their accumulation at the tumor as they express higher CCR2 and CXCR6 relative to other helper subsets (*9*, *24*). Yet, we remain cautious to dismiss the impact of CD26 itself in tumor immunity, as future work will test whether CD26 overexpression is able to improve subtherapeutic T cell products and address this concept in model systems with intact host immunity.

Beyond CD26 and IL-17, other factors within the cell product may differentiate CD26^{high} from T_H17 cell therapies. CD26^{high} T cells produced more cytotoxic molecules than T_H17 and bulk CD4$^+$ T cells and did not require CD8$^+$ T cells to instill immunity, suggesting an ability to directly lyse tumor in vivo. Further investigation revealed that sorting T_H17 cells by CCR4$^+$CCR6$^+$ yielded an IL-17$^+$ population containing FoxP3$^+$IL-2Rα^{high} T_{regs}, which was not present when sorting CD26^{high} T cells. The enrichment of polyfunctional and cytotoxic over regulatory properties in CD26^{high} T cells may support their durable responses, which provides insights on sorting functional CD4$^+$ cells for cancer immunotherapies.

Last, while our work shows that enriching CD4$^+$ T cell subsets can improve suboptimal CAR constructs lacking costimulation, it will be important to clinically elucidate the impact of costimulatory domains and cytokine support on the persistence and durability of CD4$^+$ T cell populations. Expanding the CD4$^+$ CAR product with CD3/ICOS activator beads rather than clinically standard CD3/CD28 beads enhanced IFN-γ and/or IL-17A production by T cell subsets while diminishing T_{reg} populations. Indeed, cotransfer of CD4$^+$ CAR T cells containing ICOS domains improves the persistence of CD8$^+$ T cells equipped with CD28 or 4-1BB domains (*25*). These data suggest that ICOS costimulation may enhance engraftment, persistence, and tumor immunity of CD4$^+$ CAR T cell products relative to traditional CD3/CD28 bead activation. In addition to costimulation, cytokine support may play an important role for CD4$^+$ subsets after adoptive transfer. Although all CD4$^+$ subsets described herein produced IL-2, CAR T cells were supported by exogenous IL-2 in this

model, which was used on the basis of preclinical work demonstrating the ability of IL-2 to improve function of tumor-specific T cells (*26*). RNA sequencing of human $CD4^+$ subsets revealed that $CD26^{high}$ and T_H17 cells expressed elevated IL-2Rα and IL-2Rβ transcripts, while most CD4 cells expressed IL-7Rα. While it remains possible that IL-2 promotes the engraftment of T_H17 and $CD26^{high}$ cells over others based on their surface receptor profile, it is not likely that exogenous IL-2 is critical for long-term persistence, as this cytokine was only provided for the first 3 days after ACT. We acknowledge that other costimulatory molecules or cytokines may differentially affect $CD4^+$ cell subsets, as tested here, a concept worth addressing to yield the most therapeutic T cell products for patients with a variety of malignancies.

There are many implications from our findings given the significant antitumor responses mediated by $CD26^{high}$ T cells in a mouse model of large established human mesothelioma. The epigenetic and molecular landscape of these helper subsets will permit investigators to address previously unexplored questions regarding their function in the immune system. Future work to translate, target, and redirect these cells to eradicate tumors or target cells inducing autoimmunity in the clinic could provide new treatment options for a vast array of diseases. Clinical trial designs are now underway based on our findings to evaluate the potential of $CD4^+CD26^{high}$ T cells in patients.

METHODS

Study design

Sample size: As these experiments were exploratory, there was no estimation to base the effective sample size; therefore, we based our animal studies using sample sizes ≥5. Rules for stopping data collection: Experimental end points were designated before study execution. Tumor control studies were conducted over ~70 days. Data inclusion/exclusion: For experiments reported here, animals were only excluded if tumors were very small or not measurable, a rule established prospectively before any therapy initiation. Outliers: Outliers were reported. End points: Tumor end point was reached when tumor area exceeded 400 mm^2. Remaining mice were euthanized, and spleens were harvested when more than half of the mice in a group reached tumor end point. Randomization: Before therapy, mice were randomized on the basis of tumor size. Blinding: Tumors were measured using $L \times W$ measurements via calipers by personnel blinded to the treatment group.

Statistical analysis

Tumor area results were transformed using the natural logarithm for data analysis. Mixed-effects linear regression models with a random component to account for the correlation of the repeated measure within a mouse were used to estimate tumor area over time. In circumstances where linearity assumptions were not met, polynomial regression models were used (*27*). Linear combinations of the resulting model coefficients were used to construct estimates for the slope differences with 95% confidence intervals (CIs), where applicable. For polynomial models, estimates were constructed for the differences in area between groups on the last day where at least one mouse was alive in all groups. Experiments with multiple groups were analyzed using one-way analysis of variance (ANOVA) with postcomparison of all pairwise groups using Tukey's range test. Experiments comparing two groups were analyzed using a Student's *t* test. The center values are the means. TCRβ sequencing analysis was based on the log-linear model, and the "relative risks" were calculated with a 95% CI.

Subset isolation

Deidentified, normal human donor peripheral blood cells were purchased as a buffy coat (Plasma Consultants) or leukapheresis (Research Blood Components). Peripheral blood lymphocytes (PBLs) were enriched using lymphocyte separation media (Mediatech). $CD4^+$ T cells were negatively isolated using magnetic bead separation (Dynabeads, Invitrogen) and plated in culture medium with a low concentration of rhIL-2 [20 IU/ml; National Institutes of Health (NIH) repository] overnight. For in vivo studies, $CD8^+$ T cells were positively isolated before the enrichment of $CD4^+$ T cells. The following morning, $CD4^+$ T cells were stained using PE-CD26 (BA5b), AlexaFluor647-CXCR3 (G025H7), PECy7-CCR6 (G034E3, BioLegend), FITC-CCR4 (205410, R&D Systems), and APCCy7-CD4 (OKT4, BD Pharmingen). Cells were sorted on the basis of the following gating strategies: bulk CD4:$CD4^+$; T_H1:$CD4^+CCR6^-CCR4^-CXCR3^+$; T_H2:$CD4^+CCR6^-CCR4^+CXCR3^-$; T_H17:$CD4^+CCR6^+CCR4^+$; and CD26:$CD4^+CD26^{high}$. Cells were sorted on a BD FACSAria IIu cell sorter or on a Beckman MoFlo Astrios high-speed cell sorter.

T cell culture

Human: T cell subsets were expanded in RPMI 1640 culture medium supplemented with nonessential amino acids, L-glutamine, sodium pyruvate, Hepes, penicillin/streptomycin, β-mercaptoethanol, and fetal bovine serum. Cells were cultured at either a 1:1 or 1:10 bead–to–T cell ratio. Magnetic beads (Dynabeads, Life Technologies) coated with antibodies to CD3 (OKT3) and/or ICOS (ISA-3, eBioscience) or CD28 (CD28.2, BioLegend) were produced in the laboratory according to the manufacturers' protocols. rhIL-2 (100 IU/ml; NIH repository) was added on day 2, and media were replaced as needed. For CRISPR experiments, bulk human $CD4^+$ cells were polarized to T_H17 phenotype using a cocktail of cytokines [hIL-6 (10 ng/ml), hIL-1β (10 ng/ml), hIL-23 (20 ng/ml), and αIFN-γ and αIL-4 (5 μg/ml)].

T cell transduction

To generate mesothelin-specific T cells, αCD3/ICOS-activated, sorted $CD4^+$ and bulk $CD8^+$ T cells were transduced with a lentiviral vector encoding a chimeric anti-mesothelin single-chain variable fragment fusion protein containing the TCRζ signaling domain (first-generation meso-CAR) or a truncated CD3ζ nonsignaling domain (Δζ) that was generated as described previously (*19*). CAR expression was determined using a flow cytometry antibody specific for the murine $F(ab')_2$ fragment (Jackson ImmunoResearch, 115-606-006). Cells were normalized for CAR expression before adoptive transfer.

Flow cytometry

For intracellular staining data, cells were stimulated with PMA (phorbol 12-myristate 13-acetate)/ionomycin. After 1 hour, Monensin (BioLegend) was added and incubated for another 3 hours. Following surface staining, intracellular staining with antibodies was performed according to the manufacturer's protocol using Fix and Perm buffers (BioLegend). Data were acquired on a BD FACSVerse or LSRII X-20 (BD Biosciences) and analyzed using the FlowJo software (BD Biosciences).

Microarray

RNA was isolated from sorted $CD4^+$ T cells using the Qiagen RNeasy Mini kit and frozen. RNA was submitted to the Phalanx Biotech

Group for processing on their OneArray platform (San Diego, CA). Heat map and principal components analysis clustering: Graphing was performed in R (version 3.1.2) using gplots (version 2.16.0). Log_2 values for $CD4^+$ cells were averaged and used as baseline for the genes of interest. For each individual sample, the fold change relative to baseline was calculated, and the median value for the triplicates was calculated and used for generating figures.

ATAC sequencing

Sorted $CD4^+$ T cells were cryopreserved in CryoStor and sent for analysis. Naïve cells were sorted on the basis of expression of CCR7 and CD45RA. ATAC-seq was performed by Epinomics according to the protocol described by Buenrostro *et al.* (*28*). Fifty thousand sorted T cells were frozen using Cryostor CS10 freeze media (BioLife Solutions) and shipped on dry ice for processing and analysis to Epinomics (Menlo Park, CA).

TCRβ sequencing

Sorted T cells were centrifuged and washed in phosphate-buffered saline (PBS), and genomic DNA was extracted using Wizard Genomic DNA purification kit (Promega). The quantity and purity of genomic DNA were assessed through spectrophotometric analysis using NanoDrop (Thermo Fisher Scientific). Amplification of TCR genes was done within the laboratory using the ImmunoSEQ hsTCRβ kit (Adaptive Biotechnologies Corp., Seattle, WA) according to the manual. Survey sequencing of TCRβ was performed by the Hollings Cancer Center Genomics Core using the Illumina MiSeq platform.

Single-cell RNA sequencing

Sorted T_H17, $CD26^{high}$ T cells, or bulk $CD4^+$ T cells were cryopreserved and sent for analysis to David H. Murdock Medical Research Institutes Genomics Core. Genomic DNA was analyzed using the Chromium Controller instrument (10X Genomics, Pleasanton, CA), which uses molecular barcoding to generate single-cell transcriptome data (*29*). Sequencing of the prepared samples was performed with a HiSeq2500 platform (Illumina). Data were analyzed with Long Ranger and visualized with Loupe (10X Genomics).

Mice and tumor line

NSG mice (the Jackson laboratory) were bred at the University of Pennsylvania or at the Medical University of South Carolina. NSG mice were given ad libitum access to autoclaved food and acidified water. M108 xenograft tumors (gift from C. H. June), described previously (*19*), were tested for mycoplasma during expansion (Lonza). C57BL/6 and TRP-1 TCR transgenic mice (*10*) were purchased from the Jackson laboratory and housed/bred in the comparative medicine department at the Medical University of South Carolina Hollings Cancer Center (MUSC, Charleston, SC). The B16F10 melanoma tumor cell line was gifted by N. P. Restifo from the Surgery Branch of the National Cancer Institute.

CRISPR for human T cells

Primary human T cells were activated for 3 days with aCD3/ICOS beads before CRISPR manipulation. On day 3, cells were debeaded and rested for 3 hours before electroporation. Two micrograms of CD26-specific single-guide RNA (sgRNA) (GenScript) was combined with 1 μg of GeneArt Platinum Cas9 Nuclease (Thermo Fisher Scientific) per 1×10^6 cells and incubated for 20 min at room temperature. During this time, cells were washed three times in PBS and then resuspended in T buffer (Neon Transfection Kit, Thermo Fisher Scientific) at 4×10^6 cells/100 μl. The sgRNA-Cas9 mixture was then added to the cells, followed by electroporation (2250 V, 20 ms, 1 pulse) using the Neon Transfection system (Thermo Fisher Scientific). Control cells were electroporated without the addition of sgRNA-Cas9. Cells were immediately returned to culture in prewarmed cell media without antibiotics but containing an additional 1% L-glutamine. Following an overnight rest, cells were resuspended in complete culture medium with IL-2 for normal culture.

Confocal microscopy

Human T cells were fixed in 4% paraformaldehyde at room temperature for 15 min. Following centrifugation, cells were blocked in 1% bovine serum albumin (BSA) for 20 min at room temperature. Cells were then centrifuged and stained with an unconjugated anti-CD26 primary antibody (1:50 in 1% BSA) overnight at 4°C. The following morning, T cells were washed with PBS and incubated in secondary antibody (goat-α-mouse AF647; BioLegend) for 1 hour at room temperature. After washing, cells were attached to glass slides using a Cytospin centrifuge and imaged using an Olympus Fv10i confocal microscope.

Ethics approval

Human peripheral blood was not collected specifically for the purposes of this research, and all samples were distributed to the laboratory in a deidentified manner. Therefore, this portion of our research was not subject to institutional review board (IRB) oversight. All animal studies were approved by the Institutional Animal Care and Use Committee at the Medical University of South Carolina.

SUPPLEMENTARY MATERIALS

Supplementary material for this article is available at http://advances.sciencemag.org/cgi/content/full/6/27/eaba7443/DC1

View/request a protocol for this paper from *Bio-protocol*.

REFERENCES AND NOTES

1. K. Ohnuma, N. H. Dang, C. Morimoto, Revisiting an old acquaintance: CD26 and its molecular mechanisms in T cell function. *Trends Immunol.* **29**, 295–301 (2008).
2. X. Ou, H. A. O'Leary, H. E. Broxmeyer, Implications of DPP4 modification of proteins that regulate stem/progenitor and more mature cell types. *Blood* **122**, 161–169 (2013).
3. B. Fleischer, CD26: A surface protease involved in T-cell activation. *Immunol. Today* **15**, 180–184 (1994).
4. N. H. Dang, Y. Torimoto, K. Sugita, J. F. Daley, P. Schow, C. Prado, S. F. Schlossman, C. Morimoto, Cell surface modulation of CD26 by anti-1F7 monoclonal antibody. Analysis of surface expression and human T cell activation. *J. Immunol.* **145**, 3963–3971 (1990).
5. S. M. J. Paulissen, J. P. van Hamburg, W. Dankers, E. Lubberts, The role and modulation of CCR6+ Th17 cell populations in rheumatoid arthritis. *Cytokine* **74**, 43–53 (2015).
6. M. Krakauer, P. S. Sorensen, F. Sellebjerg, CD4+ memory T cells with high CD26 surface expression are enriched for Th1 markers and correlate with clinical severity of multiple sclerosis. *J. Neuroimmunol.* **181**, 157–164 (2006).
7. K. Ohnuma, R. Hatano, T. M. Aune, H. Otsuka, S. Iwata, N. H. Dang, T. Yamada, C. Morimoto, Regulation of pulmonary graft-versus-host disease by IL-26^+CD26^+CD4 T lymphocytes. *J. Immunol.* **194**, 3697–3772 (2015).
8. I. Z. Matić, M. Đorđić, N. Grozdanić, A. Damjanović, B. Kolundžija, A. Erić-Nikolić, R. Džodić, M. Šašić, S. Nikolić, D. Dobrosavljević, S. Rašković, S. Andrejević, D. Gavrilović, O. J. Cordero, Z. D. Juranić, Serum activity of DPPIV and its expression on lymphocytes in patients with melanoma and in people with vitiligo. *BMC Immunol.* **13**, 48 (2012).
9. S. R. Bailey, M. H. Nelson, K. Majchrzak, J. S. Bowers, M. M. Wyatt, A. S. Smith, L. R. Neal, K. Shirai, C. Carpenito, C. H. June, M. J. Zilliox, C. M. Paulos, Human $CD26^{high}$T cells elicit tumor immunity against multiple malignancies via enhanced migration and persistence. *Nat. Commun.* **8**, 1961 (2017).
10. P. Muranski, A. Boni, P. A. Antony, L. Cassard, K. R. Irvine, A. Kaiser, C. M. Paulos, D. C. Palmer, C. E. Touloukian, K. Ptak, L. Gattinoni, C. Wrzesinski, C. S. Hinrichs,

K. W. Kerstann, L. Feigenbaum, C.-C. Chan, N. P. Restifo, Tumor-specific Th17-polarized cells eradicate large established melanoma. *Blood* **112**, 362–373 (2008).
11. N. Martin-Orozco, P. Muranski, Y. Chung, X. O. Yang, T. Yamazaki, S. Lu, P. Hwu, N. P. Restifo, W. W. Overwijk, C. Dong, T helper 17 cells promote cytotoxic T cell activation in tumor immunity. *Immunity* **31**, 787–798 (2009).
12. J. S. Bowers, M. H. Nelson, K. Majchrzak, S. R. Bailey, B. Rohrer, A. D. Kaiser, C. Atkinson, L. Gattinoni, C. M. Paulos, Th17 cells are refractory to senescence and retain robust antitumor activity after long-term ex vivo expansion. *JCI Insight* **2**, e90772 (2017).
13. S. H. Chang, S. G. Mirabolfathinejad, H. Katta, A. M. Cumpian, L. Gong, M. S. Caetano, S. J. Moghaddam, C. Dong, T helper 17 cells play a critical pathogenic role in lung cancer. *Proc. Natl. Acad. Sci. U.S.A.* **111**, 5664–5669 (2014).
14. E. V. Acosta-Rodriguez, L. Rivino, J. Geginat, D. Jarrossay, M. Gattorno, A. Lanzavecchia, F. Sallusto, G. Napolitani, Surface phenotype and antigenic specificity of human interleukin 17-producing T helper memory cells. *Nat. Immunol.* **8**, 639–646 (2007).
15. B. Bengsch, B. Seigel, T. Flecken, J. Wolanski, H. E. Blum, R. Thimme, Human Th17 cells express high levels of enzymatically active dipeptidylpeptidase IV (CD26). *J. Immunol.* **188**, 5438–5447 (2012).
16. S. Becattini, D. Latorre, F. Mele, M. Foglierini, C. De Gregorio, A. Cassotta, B. Fernandez, S. Kelderman, T. N. Schumacher, D. Corti, A. Lanzavecchia, F. Sallusto, Functional heterogeneity of human memory $CD4^+$ T cell clones primed by pathogens or vaccines. *Science* **347**, 400–406 (2015).
17. C. M. Paulos, C. Carpenito, G. Plesa, M. M. Suhoski, A. Varela-Rohena, T. N. Golovina, R. G. Carroll, J. L. Riley, C. H. June, The inducible costimulator (ICOS) is critical for the development of human T_H17 cells. *Sci. Transl. Med.* **2**, 55ra78 (2010).
18. T. N. Golovina, T. Mikheeva, M. M. Suhoski, N. A. Aqui, V. C. Tai, X. Shan, R. Liu, R. R. Balcarcel, N. Fisher, B. L. Levine, R. G. Carroll, N. Warner, B. R. Blazar, C. H. June, J. L. Riley, CD28 costimulation is essential for human T regulatory expansion and function. *J. Immunol.* **181**, 2855–2868 (2008).
19. C. Carpenito, M. C. Milone, R. Hassan, J. C. Simonet, M. Lakhal, M. M. Suhoski, A. Varela-Rohena, K. M. Haines, D. F. Heitjan, S. M. Albelda, R. G. Carroll, J. L. Riley, I. Pastan, C. H. June, Control of large, established tumor xenografts with genetically retargeted human T cells containing CD28 and CD137 domains. *Proc. Natl. Acad. Sci. U.S.A.* **106**, 3360–3365 (2009).
20. H. M. Knochelmann, A. S. Smith, C. J. Dwyer, M. M. Wyatt, S. Mehrotra, C. M. Paulos, CAR T cells in solid tumors: Blueprints for building effective therapies. *Front. Immunol.* **9**, 1740 (2018).
21. D. Sommermeyer, M. Hudecek, P. L. Kosasih, T. Gogishvili, D. G. Maloney, C. J. Turtle, S. R. Riddell, Chimeric antigen receptor-modified T cells derived from defined $CD8^+$ and $CD4^+$ subsets confer superior antitumor reactivity in vivo. *Leukemia* **30**, 492–500 (2015).
22. C. J. Turtle, L.-A. Hanafi, C. Berger, T. A. Gooley, S. Cherian, M. Hudecek, D. Sommermeyer, K. Melville, B. Pender, T. M. Budiarto, E. Robinson, N. N. Steevens, C. Chaney, L. Soma, X. Chen, C. Yeung, B. Wood, D. Li, J. Cao, S. Heimfeld, M. C. Jensen, S. R. Riddell, D. G. Maloney, CD19 CAR-T cells of defined $CD4^+$:$CD8^+$ composition in adult B cell ALL patients. *J. Clin. Invest.* **126**, 2123–2138 (2016).
23. P. Muranski, Z. A. Borman, S. P. Kerkar, C. A. Klebanoff, Y. Ji, L. Sanchez-Perez, M. Sukumar, R. N. Reger, Z. Yu, S. J. Kern, R. Roychoudhuri, G. A. Ferreyra, W. Shen, S. K. Durum, L. Feigenbaum, D. C. Palmer, P. A. Antony, C. C. Chan, A. Laurence, R. L. Danner, L. Gattinoni, N. P. Restifo, Th17 cells are long lived and retain a stem cell-like molecular signature. *Immunity* **35**, 972–985 (2011).
24. H. H. Zhang, K. Song, R. L. Rabin, B. J. Hill, S. P. Perfetto, M. Roederer, D. C. Douek, R. M. Siegel, J. M. Farber, CCR2 identifies a stable population of human effector memory $CD4^+$ T cells equipped for rapid recall response. *J. Immunol.* **185**, 6646–6663 (2010).
25. S. Guedan, A. D. Posey Jr., C. Shaw, A. Wing, T. Da, P. R. Patel, S. E. McGettigan, V. Casado-Medrano, O. U. Kawalekar, M. Uribe-Herranz, D. Song, J. J. Melenhorst, S. F. Lacey, J. Scholler, B. Keith, R. M. Young, C. H. June, Enhancing CAR T cell persistence through ICOS and 4-1BB costimulation. *JCI Insight* **3**, e96976 (2018).
26. W. W. Overwijk, M. R. Theoret, S. E. Finkelstein, D. R. Surman, L. A. de Jong, F. A. Vyth-Dreese, T. A. Dellemijn, P. A. Antony, P. J. Spiess, D. C. Palmer, D. M. Heimann, C. A. Klebanoff, Z. Yu, L. N. Hwang, L. Feigenbaum, A. M. Kruisbeek, S. A. Rosenberg, N. P. Restifo, Tumor regression and autoimmunity after reversal of a functionally tolerant state of self-reactive $CD8^+$ T cells. *J. Exp. Med.* **198**, 569–580 (2003).
27. N. M. Laird, J. H. Ware, Random-effects models for longitudinal data. *Biometrics* **38**, 963–974 (1982).
28. J. D. Buenrostro, P. G. Giresi, L. C. Zaba, H. Y. Chang, W. J. Greenleaf, Transposition of native chromatin for fast and sensitive epigenomic profiling of open chromatin, DNA-binding proteins and nucleosome position. *Nat Methods* **10**, 1213–1218 (2013).
29. G. X. Y. Zheng, B. T. Lau, M. Schnall-Levin, M. Jarosz, J. M. Bell, C. M. Hindson, S. Kyriazopoulou-Panagiotopoulou, D. A. Masquelier, L. Merrill, J. M. Terry, P. A. Mudivarti, P. W. Wyatt, R. Bharadwaj, A. J. Makarewicz, Y. Li, P. Belgrader, A. D. Price, A. J. Lowe, P. Marks, G. M. Vurens, P. Hardenbol, L. Montesclaros, M. Luo, L. Greenfield, A. Wong, D. E. Birch, S. W. Short, K. P. Bjornson, P. Patel, E. S. Hopmans, C. Wood, S. Kaur, G. K. Lockwood, D. Stafford, J. P. Delaney, I. Wu, H. S. Ordonez, S. M. Grimes, S. Greer, J. Y. Lee, K. Belhocine, K. M. Giorda, W. H. Heaton, G. P. McDermott, Z. W. Bent, F. Meschi, N. O. Kondov, R. Wilson, J. A. Bernate, S. Gauby, A. Kindwall, C. Bermejo, A. N. Fehr, A. Chan, S. Saxonov, K. D. Ness, B. J. Hindson, H. P. Ji, Haplotyping germline and cancer genomes with high-throughput linked-read sequencing. *Nat. Biotechnol.* **34**, 303–311 (2016).

Acknowledgments: We thank L. Stefanik, K. Schwartz, and M. Diven of the Department of Microbiology and Immunology for assistance. We thank A. Soloff and Z. McPherson at the MUSC Flow Cytometry and Cell Sorting Core and C. Fuchs at the Regenerative Medicine Department Flow Core for sorting cells. We also thank A. Smith, C. Dwyer, G. Rangel Rivera, A. Rivera-Reyes, D. Arhontoulis, E. Ansa-Addo, K. Thyagarajan, and J. Varela for critical reading and feedback. We want to acknowledge E. Garrett-Mayer for TCRβ data analysis, A. Aksoy and J. Martello for assistance with the single-cell sequencing analysis, and Epinomics for collaboration and ATAC-seq analysis. Last, we want to thank C. June (University of Pennsylvania) and N. Restifo (Surgery Branch, NCI) for reagents and support. **Funding:** This work was supported by start-up funds at MUSC, NCI R01 CA175061, NCI R01 CA 208514, American Cancer Society IRG (016623-004), and the KL2 (UL1 TR000062) to C.M.P.; Jeane B. Kempner Postdoctoral Fellowship and the American Cancer Society Postdoctoral Fellowship (122704-PF-13-084-01-LIB) to M.H.N.; NCI F30 CA243307, T32 GM008716, and T32 DE017551 to H.M.K.; NCI F31 CA192787 to S.R.B.; NIH F30 CA200272 and T32 GM008716 to J.S.B.; NCI R50 CA233186 to M.M.W.; NCI R01 CA222817 to M.P.R.; Hollings Cancer Center Flow Cytometry & Cell Sorting and the Genomics Shared Resource (P30 CA138313). **Author contributions:** M.H.N. designed and executed the experiments, analyzed the data, created the figures, and wrote and edited the manuscript; H.M.K. performed the experiments, analyzed the data, created the figures, and wrote and edited the manuscript; S.R.B., J.S.B., L.W.H., K.M.-K, and M.M.W. performed the experiments; K.E.A., P.G.G., and M.J.Z. analyzed the data; S.M., M.P.R., M.I.N., and H.E.B. designed the experiments and edited the manuscript; and C.M.P. directed the project, designed the experiments, and edited the manuscript. All authors critically read and approved the manuscript. **Competing interests:** C.M.P. has a patent for the expansion of T_H17 cells using ICOSL-expressing aAPCs. M.H.N., S.R.B., and C.M.P. have a patent for the use of $CD26^{high}$ T cells for the use in adoptive T cell transfer therapy. All the other authors declare that they have no competing interests. **Data and materials availability:** All data needed to evaluate the conclusions in the paper are present in the paper and/or the Supplementary Materials. Additional data related to this paper may be requested from the authors. For original data, please contact paulos@musc.edu. Microarray data can be found at GEO accession number GSE106726.

Submitted 31 December 2019
Accepted 18 May 2020
Published 1 July 2020
10.1126/sciadv.aba7443

Citation: M. H. Nelson, H. M. Knochelmann, S. R. Bailey, L. W. Huff, J. S. Bowers, K. Majchrzak-Kuligowska, M. M. Wyatt, M. P. Rubinstein, S. Mehrotra, M. I. Nishimura, K. E. Armeson, P. G. Giresi, M. J. Zilliox, H. E. Broxmeyer, C. M. Paulos, Identification of human $CD4^+$ T cell populations with distinct antitumor activity. *Sci. Adv.* **6**, eaba7443 (2020).